

# Supplementary Material

Title: Optimization of cervical cord atrophy measurement using a real-world multi-center dataset in Multiple Sclerosis

## Description the software methods for cervical cord segmentation

Calculation of cord area (CSA) and longitudinal cord area changes: for CSA measurements, four different software methods were used, that have previously been used in large MS cohorts (Rocca et al. 2011; Lukas et al. 2015; Prados et al. 2016, Moccia et al. 2020). The first approach was the active surface model (ASM), a semiautomatic software method commercially available with the Jim Software package ("cord finder" tool in JIM, v. 7.0 Xinapse Systems, Colchester, UK; www.xinapse.com)(Horsfield, Sala et al. 2010, Rocca, Horsfield et al. 2011), the second semiautomatic method was the watershed-segmentation method available with NeuroQlab (NQL, Fraunhofer-Mevis, Bremen, Germany; license freely available for research purposes upon request from Fraunhofer-Mevis) (Lukas, Sombekke et al. 2013, Weiler 2017). In addition to these semiautomatic approaches, two automatic software methods were chosen: the deformable model method PropSeg, and the DeepSeg tool that is based on convolutional neural networks, both freely available with the Spinal cord Toolbox (SCT) (De Leener, Kadoury et al. 2014, De Leener, Levy et al. 2017, Gros, De Leener et al. 2019) (https://spinalcordtoolbox.com).

#### ASM (JIM software):

The Active Surface tool requires interactive marking of the center of the cord at a regular distance along several vertebral levels to be included in the analysis (Horsfield, Sala et al. 2010). Cord centerline and cord outlines at each slice are then calculated using a segmentation algorithm with a steadily increasing refinement of the active surface model. This allows a rapid semi-automated segmentation by measuring the cord CSA along the length of the extracted surface. We used the cord finder tool included in JIM version 7.0, with the following settings: nominal cord diameter setting: 10 mm, number of shape coefficients: 18 and order of longitudinal variation: 5. ASM has been shown to be highly reproducible and the method has been used in previous cross sectional and in longitudinal MS studies (Rocca, Horsfield et al. 2011, Valsasina, Rocca et al. 2013, Valsasina, Rocca et al. 2015, Rocca, Valsasina et al. 2019, Weeda, Middelkoop et al. 2019, Bischof, Papinutto et al. 2022, Valsasina, Gobbi et al. 2022).

#### NQL:

NQL (version 4.01) requires as the first step to define interactively the section of the cord to be analysed by placing an oblique plane through the dataset, which runs through the upper and lower end of the section (Weiler 2017). This is aided by two perpendicular lines, which allow precise alignment of the section to the specific vertebral bodies. This step is followed by a semi-automatic pre-segmentation using a watershed transformation of the pixel intensities. Subsequently, a fully automated model based volume measurement is performed by fitting the intensity distribution of the pre-segmented input region using a Gaussian mixture model. The spinal cord volume is modelled using Gaussian mixture of two tissue classes (spinal cord tissue and CSF) and a separate class

representing partial volume voxels. The volume is calculated by summation of the spinal cord tissue class volume and half of the volume of the partial volume class. The center-line of the SC is calculated and used to determine the mean CSA by normalizing the measured volume to the section length. The operator can correct the final results interactively. NQL has been shown to be highly reproducible (Lukas, Sombekke et al. 2013, Weiler 2017) and the method has already been used in cross-sectional and in longitudinal studies of different neurological diseases including MS (Lukas, Hahn et al. 2008, Daams, Weiler et al. 2014, Lukas, Knol et al. 2015, Liu, Lukas et al. 2016, Schneider, Bellenberg et al. 2017, Wilhelms, Bellenberg et al. 2017, Weeda, Middelkoop et al. 2019).

#### SCT PropSeg (SCT\_PS)

The Spinal Cord Toolbox SCT features specific segmentation tools for the spinal cord. The segmentation algorithm PropSeg is based on an iterative propagation of a deformable model with adaptive contrast mechanism (De Leener, Kadoury et al. 2014, De Leener, Levy et al. 2017). Automated detection of the center of the spinal cord is done by ellipse detection and information from the body symmetry, followed by propagating a tubular surface along the spinal cord edge using deformable models. SCT\_PS has been applied in studies on MS patients (Yiannakas, Mustafa et al. 2016) and has been shown to be highly reproducible (McCoy, Dupont et al. 2019).

# SCT DeepSeg (SCT\_DS)

The DeepSeg algorithm implemented in SCT is based on a deep learning convolutional neural network (CNN) module trained to effectively segment the spinal cord from MRI images. SCT\_DS was trained from masks generated by SCT\_PS, which were manually corrected if necessary (De Leener, Levy et al. 2017, Gros, De Leener et al. 2019). SCT\_DS has been thoroughly evaluated in a large multi-centre dataset of HC and has been applied in different diseases related to cord atrophy (McCoy, Dupont et al. 2019, Moccia, Valsecchi et al. 2020, Bautin and Cohen-Adad 2021).

We used SCT (version 5.6, https://spinalcordtoolbox.com) with default settings to segment the cervical cord and automatically identify different vertebral levels in SCT\_PS and SCT\_DS. The segmentation and labeling quality was visually inspected using the implemented quality control tool. Problems with automatic vertebral labeling in single cases were resolved by using the dedicated manual labeling procedure.

#### Average operator times required for a single CSA measurement

For the semiautomated methods ASM and NQL, although the computation times for spinal cord segmentation are fast (< 1 min), average operator times for a single CSA measurement including potential error correction, and estimation of normalization measures are 8-10 minutes.

For the automated methods of Spinal Cord Toolbox SCT\_DS and SCT\_PS the speed of the spinal cord segmentation and output of results directly depends on the computing power of the system used and for example takes 7 minutes for cord segmentation using a standalone computer equipped with quad-core Intel Core i5 64-bit 1.4 GHz CPU and Memory 8 GB 2133 MHz. After automatic processing of a bulk of examinations additional operator time of 2-3 minutes per scan is required for quality control and estimation of normalization measures.

#### Consideration of partial volume effects and of cord curvature in the different software methods:

As laid out in detail in our previous methodological study, the methods have specific differences related to the definition of the cord edges and handling of partial volume effects at the transition between cord and surrounding cerebrospinal fluid (CSF)(Lukas, Bellenberg et al. 2021). In addition, the effects of cord curvature are treated differently between ASM and NQL or SCT\_PS and SCT\_DS. Due to the limited image resolution and the small diameter of the SC these effects may account for a substantial proportion of the segmented volume (Yiannakas, Mustafa et al. 2016, Weeda, Middelkoop et al. 2019, Lukas, Bellenberg et al. 2021).

The SCT\_PS algorithm includes only voxels into the segmentation that are classified as "pure" cord tissue, without referring to partial volume effects at the margin of the cord contour. As SCT\_DS segmentation was trained on SCT\_PS results, the method has the same characteristic as SCT\_PS and excludes voxels that are prone to partial volume effects. In contrast, NQL includes pure cord tissue voxels and 50% of the partial-volume tissue class in the CSA calculation (Weiler 2017, Yiannakas, Mustafa et al. 2016). Similarly to NQL, the cord segmentation of ASM includes a fraction of those voxels subject to partial volume effects between the cord and the surrounding CSF because the cord surface definition is partly controlled by seeking high intensity gradients (Horsfield, Sala et al. 2010). Thus, CSA results of ASM and NQL are typically higher than CSA generated by SCT\_PS or SCT\_DS.

Additionally, effects of the cervical cord curvature are treated differently between NQL and ASM or SCT. While ASM and SCT methods are optimized with regards to variations of the cord curvature (Horsfield, Sala et al. 2010, De Leener, Kadoury et al. 2014), NQL quantifies the cord volume between two parallel oblique planes, and uses the centerline merely for calculation of the mean cord area from the segmented volume (Weiler 2017). Thus, the CSA estimations by NQL might differ from the corresponding ASM or SCT results, depending of the degree of curvature of the SC, or the exact choice of the cord section to be analyzed.

#### **References (Supplement)**

Bautin, P. & Cohen-Adad, J. 2021. Minimum detectable spinal cord atrophy with automatic segmentation: Investigations using an open-access dataset of healthy participants. Neuroimage Clin, 32, 102849.

Bischof, A., Papinutto, N., Keshavan, A., Rajesh, A., Kirkish, G., Zhang, X., Mallott, J. M., Asteggiano, C., Sacco, S., Gundel, T. J., Zhao, C., Stern, W. A., Caverzasi, E., Zhou, Y., Gomez, R., Ragan, N. R., Santaniello, A., Zhu, A. H., Juwono, J., Bevan, C. J., Bove, R. M., Crabtree, E., Gelfand, J. M., Goodin, D. S., Graves, J. S., Green, A. J., Oksenberg, J. R., Waubant, E., Wilson, M. R., Zamvil, S. S., University of California, S. F. M. S. E. T., Cree, B. a. C., Hauser, S. L. & Henry, R. G. 2022. Spinal Cord Atrophy Predicts Progressive Disease in Relapsing Multiple Sclerosis. Ann Neurol, 91, 268-281.

Daams M, Weiler F, Steenwijk MD, Hahn HK, Geurts JJ, Vrenken H, et al. Mean upper cervical cord area (MUCCA) measurement in long-standing multiple sclerosis: relation to brain findings and clinical disability. Mult Scler J. (2014) 20:1860–5.

De Leener, B., Kadoury, S. & Cohen-Adad, J. 2014. Robust, accurate and fast automatic segmentation of the spinal cord. Neuroimage, 98, 528-36.

De Leener, B., Levy, S., Dupont, S. M., Fonov, V. S., Stikov, N., Louis Collins, D., Callot, V. & Cohen-Adad, J. 2017. SCT: Spinal Cord Toolbox, an open-source software for processing spinal cord MRI data. Neuroimage, 145, 24-43.

Gros, C., De Leener, B., Badji, A., Maranzano, J., Eden, D., Dupont, S. M., Talbott, J., Zhuoquiong, R., Liu, Y., Granberg, T., Ouellette, R., Tachibana, Y., Hori, M., Kamiya, K., Chougar, L., Stawiarz, L., Hillert, J., Bannier, E., Kerbrat, A., Edan, G., Labauge, P., Callot, V., Pelletier, J., Audoin, B., Rasoanandrianina, H., Brisset, J. C., Valsasina, P., Rocca, M. A., Filippi, M., Bakshi, R., Tauhid, S., Prados, F., Yiannakas, M., Kearney, H., Ciccarelli, O., Smith, S., Treaba, C. A., Mainero, C., Lefeuvre, J., Reich, D. S., Nair, G., Auclair, V., Mclaren, D. G., Martin, A. R., Fehlings, M. G., Vahdat, S., Khatibi, A., Doyon, J., Shepherd, T., Charlson, E., Narayanan, S. & Cohen-Adad, J. 2019. Automatic segmentation of the spinal cord and intramedullary multiple sclerosis lesions with convolutional neural networks. Neuroimage, 184, 901-915.

Horsfield, M. A., Sala, S., Neema, M., Absinta, M., Bakshi, A., Sormani, M. P., Rocca, M. A., Bakshi, R. & Filippi, M. 2010. Rapid semi-automatic segmentation of the spinal cord from magnetic resonance images: application in multiple sclerosis. Neuroimage, 50, 446-55.

Liu, Y., Lukas, C., Steenwijk, M. D., Daams, M., Versteeg, A., Duan, Y., Li, K., Weiler, F., Hahn, H. K., Wattjes, M. P., Barkhof, F. & Vrenken, H. 2016. Multicenter Validation of Mean Upper Cervical Cord Area Measurements from Head 3D T1-Weighted MR Imaging in Patients with Multiple Sclerosis. AJNR Am J Neuroradiol, 37, 749-54.

Lukas, C., Knol, D. L., Sombekke, M. H., Bellenberg, B., Hahn, H. K., Popescu, V., Weier, K., Radue, E. W., Gass, A., Kappos, L., Naegelin, Y., Uitdehaag, B. M., Geurts, J. J., Barkhof, F. & Vrenken, H. 2015. Cervical spinal cord volume loss is related to clinical disability progression in multiple sclerosis. J Neurol Neurosurg Psychiatry, 86, 410-8.

Lukas, C., Bellenberg, B., Prados, F., Valsasina, P., Parmar, K., Brouwer, I., Pareto, D., Rovira, A., Sastre-Garriga, J., Gandini Wheeler-Kingshott, C. a. M., Kappos, L., Rocca, M. A., Filippi, M., Yiannakas, M., Barkhof, F. & Vrenken, H. 2021. Quantification of Cervical Cord Cross-Sectional Area: Which Acquisition, Vertebra Level, and Analysis Software? A Multicenter Repeatability Study on a Traveling Healthy Volunteer. Front Neurol, 12, 693333.

Lukas, C., Hahn, H. K., Bellenberg, B., Hellwig, K., Globas, C., Schimrigk, S. K., Koster, O. & Schols, L. 2008. Spinal cord atrophy in spinocerebellar ataxia type 3 and 6: impact on clinical disability. J Neurol, 255, 1244-9.

Lukas, C., Sombekke, M. H., Bellenberg, B., Hahn, H. K., Popescu, V., Bendfeldt, K., Radue, E. W., Gass, A., Borgwardt, S. J., Kappos, L., Naegelin, Y., Knol, D. L., Polman, C. H., Geurts, J. J., Barkhof, F. & Vrenken, H. 2013. Relevance of spinal cord abnormalities to clinical disability in multiple sclerosis: MR imaging findings in a large cohort of patients. Radiology, 269, 542-52.

McCoy DB, Dupont SM, Gros C, Cohen-Adad J, Huie RJ, Ferguson A, Duong-Fernandez X, Thomas LH, Singh V, Narvid J, Pascual L, Kyritsis N, Beattie MS, Bresnahan JC, Dhall S,

Whetstone W, Talbott JF; TRACK-SCI Investigators. Convolutional Neural Network-Based Automated Segmentation of the Spinal Cord and Contusion Injury: Deep Learning Biomarker Correlates of Motor Impairment in Acute Spinal Cord Injury. AJNR Am J Neuroradiol. 2019 Apr;40(4):737-744.

Moccia, M., Valsecchi, N., Ciccarelli, O., Van Schijndel, R., Barkhof, F. & Prados, F. 2020. Spinal cord atrophy in a primary progressive multiple sclerosis trial: Improved sample size using GBSI. Neuroimage Clin, 28, 102418.

Prados, F., Cardoso, M. J., Yiannakas, M. C., Hoy, L. R., Tebaldi, E., Kearney, H., Liechti, M. D., Miller, D. H., Ciccarelli, O., Wheeler-Kingshott, C. A. & Ourselin, S. 2016. Fully automated grey and white matter spinal cord segmentation. Sci Rep, 6, 36151.

Rocca, M. A., Horsfield, M. A., Sala, S., Copetti, M., Valsasina, P., Mesaros, S., Martinelli, V., Caputo, D., Stosic-Opincal, T., Drulovic, J., Comi, G. & Filippi, M. 2011. A multicenter assessment of cervical cord atrophy among MS clinical phenotypes. Neurology, 76, 2096-102.

Rocca, M. A., Valsasina, P., Meani, A., Gobbi, C., Zecca, C., Rovira, A., Montalban, X., Kearney, H., Ciccarelli, O., Matthews, L., Palace, J., Gallo, A., Bisecco, A., Gass, A., Eisele, P., Lukas, C., Bellenberg, B., Barkhof, F., Vrenken, H., Preziosa, P., Comi, G., Filippi, M. & Group, M. S. 2019. Clinically relevant cranio-caudal patterns of cervical cord atrophy evolution in MS. Neurology, 93, e1852-e1866.

Schneider R, Bellenberg B, Kleiter I, Gold R, Köster O, Weiler F, et al. Cervical cord and ventricle affection in neuromyelitis optica. Acta Neurol Scand. (2017) 135:324–31. doi: 10.1111/ane.12601

Valsasina P, Gobbi C, Zecca C, Rovira A, Sastre-Garriga J, Kearney H, Yiannakas M, Matthews L, Palace J, Gallo A, Bisecco A, Gass A, Eisele P, Filippi M, Rocca MA; MAGNIMS Study Group;. Characterizing 1-year development of cervical cord atrophy across different MS phenotypes: A voxel-wise, multicentre analysis. Mult Scler. 2022 May;28(6):885-899.

Valsasina, P., Rocca, M. A., Horsfield, M. A., Absinta, M., Messina, R., Caputo, D., Comi, G. & Filippi, M. 2013. Regional cervical cord atrophy and disability in multiple sclerosis: a voxel-based analysis. Radiology, 266, 853-61.

Valsasina P, Rocca MA, Horsfield MA, Copetti M, Filippi M. A longitudinal MRI study of cervical cord atrophy in multiple sclerosis. J Neurol. (2015) 262:1622–8. doi: 10.1007/s00415-015-7754-z

Weeda, M. M., Middelkoop, S. M., Steenwijk, M. D., Daams, M., Amiri, H., Brouwer, I., Killestein, J., Uitdehaag, B. M. J., Dekker, I., Lukas, C., Bellenberg, B., Barkhof, F., Pouwels, P. J. W. & Vrenken, H. 2019. Validation of mean upper cervical cord area (MUCCA) measurement techniques in multiple sclerosis (MS): High reproducibility and robustness to lesions, but large software and scanner effects. Neuroimage Clin, 24, 101962.

Weiler, F., Hallmann, M. F., Schwier, M., Hildebrandt, H., Gregori, J., Spiess, L., Klein, J. & Heldmann, S. 2017. Fully automated detection, segmentation and quantification of mean cross-sectional area of the spinal cord. Multiple Sclerosis Journal, 23, 149-150.

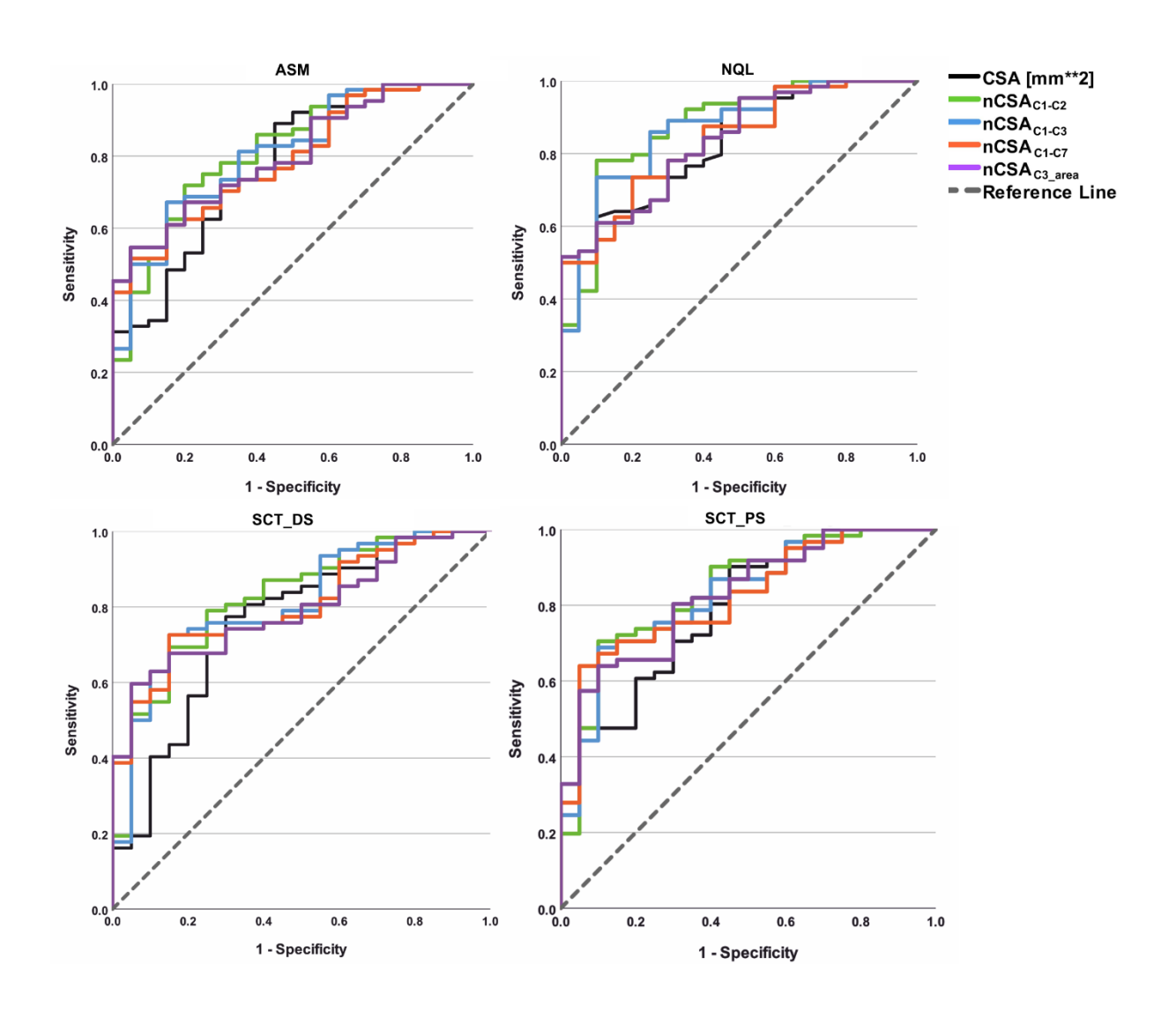
Wilhelms W, Bellenberg B, Koster O, Weiler F, Hoffmann R, Gold R, et al. Progressive spinal cord atrophy in manifest and premanifest huntington's disease. J Neurol Neurosurg Psychiatry. (2017) 88:614–6.

Yiannakas, M. C., Mustafa, A. M., De Leener, B., Kearney, H., Tur, C., Altmann, D. R., De Angelis, F., Plantone, D., Ciccarelli, O., Miller, D. H., Cohen-Adad, J. & Gandini Wheeler-Kingshott, C. A. 2016. Fully automated segmentation of the cervical cord from T1-weighted MRI using PropSeg: Application to multiple sclerosis. Neuroimage Clin, 10, 71-7.

## **Supplementary Figures and Tables**

# **Supplementary Figures**

**Supplementary Figure S1:** Example of receiver operating characteristic (ROC) curves for the differentiation between rMS and pMS using unnormalized or normalized CSA measured at the C1-7 vertebral level using the method ASM and NQL (upper row), SCT\_DS and SCT\_PS (lower row); color coding: black: unnormalized CSA, green: C1-C2 normalized CSA (nCSA $_{C1-C2}$ ), blue: C1-C3 normalized CSA (nCSA $_{C1-C3}$ ), orange: C1-C7 normalized CSA (nCSA $_{C1-C2}$ ), green: C1-C2 normalized CSA (nCSA $_{C1-C2}$ ), purple: C3-area normalized CSA (nCSA $_{C3-area}$ )



**Supplementary Tables** 

**Supplementary Table S1:** Sequence parameters of 3D-T1w imaging used with the 3Tesla scanners at the participating centers

Site Nr	1	2	3	4	5		
Vendor	GE Discovery MR750	Siemens Trio Tim	Philips Achieva	Philips Intera	Philips Achieva		
Magnet length / bore diameter [cm]	194 /60	198 / 60	157 / 60	157 / 60	157 / 60		
Coil type	HNS array 16 ch.	head-neck array 16 ch.	SENSE-NV- 16 ch.	SENSE- NV-16 ch.	SENSE-NV- 16 ch.		
Head MRI (3D-T1-v	veighted)						
Sequence	FSPGR	MPRAGE	TFE	TFE	TFE		
Number of Slices	172	192	180	204	180		
Orientation	sagittal	sagittal	Sagittal	Sagittal	sagittal		
TR (ms)	7.8	2300	10	7.1	6.8		
TE (ms)	3	3	4.6	3.2	3.1		
TI (ms)	450	900	1000	900	825		
FA	12°	9°	8°	9°	8°		
Voxel Size (mm)	0.98×0.98×1	1×1×1	1x1x1	1x1x1	1x1x1		
Cervical cord MRI (	Cervical cord MRI (3D-T1-weighted)						
Sequence	FSPGR	MPRAGE	TFE	TFE	TFE		
Number of Slices	172	128	64	64	128		
Orientation	sagittal	sagittal	sagittal	sagittal	sagittal		

TR (ms)	7.3	2300	8	8	8
TE (ms)	3	3.26	3.5	3.5	3.7
TI (ms)	450	900	1000	1000	856
FA	15°	9°	8°	8°	8°
Voxel Size (mm)	1×1×1	1×1×1	1x1x1	1x1x1	1x1x1

**Abbreviations:** TR Repetition time; TE Echo time. TI Inversion time; FA Flip angle; TFE Turbo field echo; MPRAGE Magnetization prepared rapid acquisition gradient echo; FSPGR Fast spoiled gradient recalled echo; Site Numbers: 1= Amsterdam UMC, Amsterdam; 2= Hospital Universitari Vall d'Hebron Barcelona; 3= Ruhr-University of Bochum; Bochum; 4= IRCCS San Raffaele Scientific Institute; Milano; 5= University College London; London.





**Supplementary Table S2:** Cord cross-sectional area (CSA unnormalized) in MS subgroups and HC for different software, cervical cord levels and brain or cord MRI. P-value and effect size calculations between groups were adjusted for center, age and sex.

	method	1	ASM		1	NQL		1	SCT_PS		1	SCT_DS	
n ± SD	vertebral level	C1-2	C1-2	C1-7	C1-2	C1-2	C1-7	C1-2			C1-2	C1-2	C1-7
] mean	MRI type	brain	cervical cord	cervical cord									
[mm²]	НС	$82.4 \pm 9.6$	83.9 ± 11.1	79.1± 9.9	$82.7 \pm 9.6$	$82.4 \pm 9.6$	$82.7 \pm 9.5$	$72.4 \pm 7.0$	$74.0 \pm 7.8$	$74.8 \pm 9.0$	$68.2 \pm 7.6$	$64.5 \pm 8.0$	$62.9 \pm 8.5$
드	MS	$75.4 \pm 9.1$	$76.6 \pm 9.7$	$72.6 \pm 9.7$	$75.0 \pm 9.3$	$76.0 \pm 10.0$	$76.0 \pm 10.7$	$66.3 \pm 8.9$	$68.5 \pm 10.3$	$69.6 \pm 11.9$	$61.5 \pm 8.8$	$60.5 \pm 9.1$	$58.8 \pm 8.2$
CSA	rMS	$77.0 \pm 8.5$	$78.4 \pm 9.1$	$74.9 \pm 8.5$	$77.1 \pm 8.7$	$78.4 \pm 8.9$	$79.1 \pm 8.6$	$67.9 \pm 8.5$	$70.5 \pm 9.7$	$72.7 \!\pm 10.7$	63.4± 8.3	$62.3 \pm 8.7$	$60.7 \pm 7.3$
	pMS	$70.2 \pm 8.9$	$70.9 \pm 9.6$	$65.3 \pm 9.6$	$68.2 \pm 8.0$	$68.0 \pm 9.3$	$66.0 \pm 10.6$	$61.3 \pm 8.6$	$62.4 \pm 9.8$	$59.9 \pm 10.8$	$55.8 \pm 8.0$	$54.9 \pm 8.1$	$52.8 \pm 8.1$
MS	p (HC-MS)	0.12	0.12	0.12	0.12	0.197	0.275	0.12	0.236	0.549	0.12	0.185	0.129
HC - L	Effect size η2 (95% CI)	0.07 (0.00;0.25)	0.08 (0.00;0.25)	0.07 (0.00;0.24)	0.09 (0.00;0.26)	0.04 (0.00;0.19)	0.03 (0.00;0.17)	0.07 (0.00;1.0)	0.03 (0.00;0.92)	0.01 (0.00;0.12)	0.10 (0.00;0.27)	0.05 (0.00;0.21)	0.06 (0.00;0.23)
	p (HC-pMS) <sup>a</sup>	0.024	0.08	0.034	0.012	0.021	0.012	0.062	0.366	0.344	0.021	0.096	0.096
S	Effect size η2 (95% CI)	0.32 (0.06;0.55)	0.28 (0.01;0.56)	0.34 (0.05;0.59)	0.41 (0.15;0.61)	0.37 (0.09;0.60)	0.44 (0.17;0.64)	0.29 (0.02;0.55)	0.15 0.01;0.48)	0.18 (0.01;0.53)	0.37 (0.10;0.59)	0.22 (0.0;0.53)	0.29 (0.00;0.59)
pMS	p (HC-rMS) <sup>a</sup>	0.566	0.566	0.566	0.566	0.888	0.999	0.556	0.888	0.999	0.556	0.888	0.739
rMs -	Effect size η2 (95% CI)	0.07 (0.00;0.25)	0.07 (0.00;0.23)	0.05 (0.00;0.21)	0.07 (0.00;0.24)	0.03 (0.01;0.17)	0.02 (0.0;0.15)	0.06 (0.00;0.23)	0.03 (0.00;0.17)	0.04 (0.00;0.11)	0.10 (0.00;0.27)	0.03 (0.00;0.18)	0.04 (0.00;0.20)
HC -	p (rMS- pMS) <sup>a</sup>	0.196	0.458	0.196	0.084	0.084	0.048	0.405	0.917	0.458	0.196	0.458	0.458
	Effect size η2 (95% CI)	0.15 (0.00;0.25)	0.11 (0.00;0.40)	0.19 (0.00;0.46)	0.24 (0.03;0.46)	0.27 (0.04;0.50)	0.36 (0.12;0.56)	0.12 (0.00;0.39)	0.06 (0.00;0.37)	0.14 (0.00;0.48)	0.16 (0.00;0.46)	0.11 (0.00;0.42)	0.15 (0.00;0.47)

**Abbreviations**: HC healthy controls, rMS relapsing MS, pMS progressive MS, SCT\_DS SCT\_deepseg, SCT\_PS SCT\_propseg, NQL NeuroQLab, ASM active surface method. **p:** all p-values extracted by linear mixed effect models adjusting for age and sex with center as

random intercept; **a**: pairwise contrast with Bonferroni correction for MS subgroup analyses; all p-values corrected for multiple comparisons between methodologies (Benjamini-Holm correction across methods, MRI type, vertebral level); p-values < 0.05 are marked in bold font; Effect size  $\eta^2$ : partial eta squared of CSA differences between groups.

**Supplementary Table S3:** Linear regression (general linear model) with CSA or EDSS as dependent variables with inclusion of age as covariate, sex (male=0, female=1) as fixed factor and scanner (center no. 1,2,3,4,5) as a random factor.

	HC				MS			MS	
		CSA		(	CSA		EDSS		
Parameter	Regression Coefficient B	Std Error	р	Regression Coefficient B	Std Error	р	Regression Coefficient B	Std Error	р
constant	79.18	10.701	<0.001	61.78	6.827	<0.001	3.29	1 015	0.002
age [years]	-0.032	0.323		-0.066	0.103		0.05		0.002
sex	-1.64	8.386	0.848	15.57	4.669	0.001	0.36	0.696	0.61
[center=1]	-0.74	10.981	0.947	14.94	4.675	0.002	-2.42	0.697	0.001
[center=2]	n.a.	n.a.	n.a.	19.04	5.057	<0.001	-3.36	0.754	<0.001
[center=3]	15.56	9.14	0.114	17.51	5.477	0.002	-3.02	0.801	< 0.001
[center=4]	0	n.a.	n.a.	16.44	4.685	0.001	-1.75	0.699	0.014
[center=5]	n.a.	n.a.	n.a.	0	n.a.	n.a.	0	n.a.	n.a.

Abbreviations: HC: healthy controls, MS: multiple sclerosis, Std.: standard, p: significance, n.a.: not applicable.



**Supplementary Table S4:** Comparison between unnormalized cord cross-sectional area (CSA) using different software methods, separately for brain or cord MRI at different vertebral levels (repeated measure ANOVA with 4 software methods as within-subject factor and Bonferroni correction for multiple comparisons)

MRI type	Brain MRI		Cord MRI		Cord MRI	
vertebral level	C1-2		C1-2		C1-7	
Pairwise comparison	Mean CSA difference	Sig.	Mean CSA difference	9-		Sig.
	[95% CI]		[95% CI]		[95% CI]	
SCT_DS vs. SCT_PS	-4.80	<0.001	-8.69	<0.001	-11.59	<0.001
	[-5.91;-3.70]		[-10.65-6.72]		[-14.17;-9.01]	
SCT_DS vs. NQL	-13.51	<0.001	-15.77	-15.77 <0.001		<0.001
	[-14.42;-12.60]		[-17.03;-14.52]		[-19.46;-16.30]	
SCT_DS vs. ASM	-14.31	<0.001	-16.70	<0.001	-14.48	<0.001
	[-15.17;-13.46]		[-17.82;-15.57]		[-15.65;-13.30]	
SCT_PS vs. NQL	-8.71	<0.001	-7.09	<0.001	-6.29	<0.001
	[-10.05;-7.36]		[-8.87;-5.31]		[-8.51;-4.07]	
SCT_PS vs. ASM	-9.51	<0.001	-8.01	<0.001	-2.89	0.003
	[-10.79;-8,24]		[-9.90;-6.11]		[-5.02;-0.75]	
NQL vs. ASM	-0.81	0.065	-0.92	0.038	-3.40	<0.001
	[-1.64;0.03]		[-1.81;-0.03]		[-4.64;-2.17]	

**Abbreviations:** SCT\_DS SCT\_deepseg, SCT\_PS SCT\_propseg, NQL NeuroQLab, ASM active surface method, vs: versus. Sig: p-values of pairwise comparisons using repeated measure ANOVA with 4 software methods as within-subject factor and Bonferroni correction for multiple comparisons; CI: confidence interval.

**Supplementary Table S5:** Comparison of cord cross-sectional area (CSA, unnormalized), **between brain and cord MRI** at the C1-2 vertebral level in MS and HC for different software methods.

method / vertebral level	MRI type	<b>CSA [</b> i mean ± standa	
ASM		MS	НС
C1-2	Brain vs. Cord	75.4 ± 9.1 vs. 76.6 ± 9.7	82.4 ± 9.6 vs. 83.9 ± 11.1
Paired t-test	р	<0.001	0.076
Intra-class correlation	ICC [95% CI]	0.979 [0.951;0.989]	0.992 [0.973;0.997]
NQL		MS	HC
C1-2	Brain vs. Cord	$75.0 \pm 9.3$ vs. $76.0 \pm 10.0$	82.7 ± 9.6 vs. 82.4 ± 9.6
Paired t-test	р	<0.001	0.063
Intra-class correlation	ICC [95% CI]	0.980 [0.964;0.989]	0.994 [0.981;0.998]
SCT_PS		MS	HC
C1-2	Brain vs. Cord	66.3 ± 8.9 vs. 68.5 ± 10.3	$72.4 \pm 7.0$ vs. $74.0 \pm 7.8$
Paired t-test	р	<0.001	0.232
Intra-class correlation	ICC [95% CI]	0.860 [0.728;0.922]	0.543 [-2.04;0.832]
SCT_DS		MS	HC
C1-2	Brain vs. Cord	61.5 ± 8.8 vs. 60.5 ± 9.1	68.2 ± 7.6 vs. 64.5 ± 8.0
Paired t-test	р	0.023	0.007
Intra-class correlation	ICC [95% CI]	0.957 [0.931;0.973]	0.947 [0.760;0.984]

**Abbreviations:** HC healthy controls, MS Multiple Sclerosis, pMS progressive MS, SCT\_DS SCT\_deepseg, SCT\_PS SCT\_propseg, NQL NeuroQLab, ASM active surface method. **p:** p-values: paired t-tests; ICC: intra-class correlation coefficients (two-way mixed effects model for absolute agreement and 95% confidence interval CI)

## **Supplementary Table S6: Normalization measures:**

Four different normalization measures were derived from a mid-sagittal view of the 3D-T1w cord MRI for each participant at each visit: (1) the height of the C1/C2 vertebra, measured from the tip of C1 to the lower border of the C2 vertebral body in the middle of its anterior-posterior extension; (2) the height of the C1-C3 vertebrae, measured as (1) but down to the lower border of C3 instead of C2; (3) the entire cervical cord length (C1-C7), extracted from the output of the ASM method; and (4) the area of the C3 vertebra. The vertebral heights and dimensions were measured using the ITK-SNAP software viewer (available at <a href="www.itksnap.org">www.itksnap.org</a>). Table S4 shows mean (standard deviation) values of the normalization measures within each group.

Table S4: Normalization measures within each group shown as mean (standard deviation)

Vertebral measure	HC	rMS	pMS	p-value
height C1-C2 [mm]	35.1 (3.0)	33.7 (2.9 )	35.4 (2.3 )	0.274
height C1-C3 [mm]	53.0 (4.2 )	50.6 (4.4 )	52.9 (3.8 )	0.172
height C1-C7 [mm]	125.7 (9.2 )	119.3 (10.8)	122.2 (9.2 )	0.043
area C3 [mm²]	228.6 (33.8)	202.0 (40.6 )	227.1 (49.8)	0.035

Abbreviations: HC healthy controls, rMS relapsing MS, pMS progressive MS.

p-values: between-group differences extracted by using analyses of variance (ANCOVA) adjusting for age and sex, using Bonferroni correction for multiple comparisons between subgroups.

In the ANCOVA analyses the differences in the normalization measures between groups were not significant for the height of C1-C2 and height of C1-C3, but significant for height of C1-C7 and the area of C3. There were no between-subjects effects of age, while effects of sex had a significant impact on differences between the groups. This was in line by lower values of the normalization measures in the rMS group, which had a higher fraction of female participants.

**Supplementary Table S7:** Pearson's correlation analyses between unnormalized CSA and the normalization measures in the HC group

CSA method	Pearson's correlation	height C1-C2 [mm]	height C1-C3 [mm]	height C1-C7 [mm]	area C3 [mm²]
	r	0.490	0.395	0.284	-0.217
ASM	[95% CI]	[0.187;0.708]	[0.071;0.643]	[-0.054;0.584]	[-0.513;0.125]
	p	0.003	0.019	0.098	0.210
	r	0.626	0.557	0.450	-0.090
NQL	[95% CI]	[0.375;0.792]	[0.280;0.749]	[0.142;0.678]	[-0.407;0.246]
	p	< 0.001	< 0.001	0.006	0.602
	r	0.435	0.462	0.436	0.009
SCT_PS	[95% CI]	[0.129;0.665]	[0.162;0.683]	[0.130;0.666]	[-0.316;0.332]
	p	0.007	0.004	0.007	0.957
	r	0.541	0.456	0.352	-0.089
SCT_DS	[95% CI]	[0.253;0.741]	[0.145;0.685]	[0.021;0.613]	[0.410;0.251]
	р	< 0.001	< 0.001	0.038	0.610

**Abbreviations:** SCT\_DS SCT\_deepseg, SCT\_PS SCT\_propseg, NQL NeuroQLab, ASM active surface method. p: p-values and r: coefficients of Pearson correlations; CI: confidence interval.



**Supplementary Table S8:** Receiver operating characteristic (ROC) analyses of differentiating between rMS and pMS subtypes regarding contrasts between normalized and unnormalized CSA x C1-2 and C1-7 levels x brain and cord MRI x NQL and ASM methods. We show the area under the curve (AUC), 95% confidence interval (CI) and corrected p-values of pair-wise differences between AUC. All p-values derived from pairwise AUC comparisons using DeLong's testing were corrected for multiple comparisons across all contrasts using Benjamini-Hochberg correction.

	Method		NQL			ASM	
	Vertebral Level	C1-2	C1-2	C1-7	C1-2	C1-2	C1-7
	MRI type	brain	cervical cord	cervical cord	brain	cervical cord	cervical cord
	AUC	0.771	0.791	0.832	0.692	0.716	0.770
	CI (95%)	[0.655,0.888]	[0.681,0.901]	[0.737,0.926]	[0.559,0.826]	[0.586,0.846]	[0.648,0.891]
	<b>p</b> csa/csanorm	-	-	-	-	-	-
CSA	P <sub>C1-2 / C1-7</sub>	-	0.289	-	-	0.179	-
	P brain / cord	0.290	-	-	0.370	-	-
	P <sub>NQL/ASM</sub>	0.050	.046*	0.064	-	-	-
	AUC	0.840	0.852	0.877	0.769	0.777	0.814
	CI (95%)	[0.738,0.942]	[0.751,0.952]	[0.786,0.968]	[0.645,0.893]	[0.651,0.902]	[0.706,0.922]
	<b>p</b> csa/csanorm	0.367	0.370	0.455	0.367	0.370	0.455
nCSA <sub>C1-C2</sub>	P <sub>C1-2 / C1-7</sub>	-	0.370	-	-	0.370	-
	P brain / cord	0.431	-	-	0.691	-	-
	P NQL/ASM	0.070	0.064	0.064	=	-	-
	AUC	0.837	0.843	0.866	0.770	0.769	0.807
	CI (95%)	[0.737,0.936]	[0.744,0.942]	[0.775,0.956]	[0.648,0.893]	[0.645,0.892]	[0.701,0.913]
nCSA <sub>C1-C3</sub>	<b>p</b> csa/csanorm	0.367	0.431	0.570	0.367	0.431	0.564
	P <sub>C1-2 / C1-7</sub>	-	0.370	-	-	0.370	-

	P brain / cord	0.616	-	-	0.961	-	-
	P <sub>NQL/ASM</sub>	0.138	0.138	0.064	-	-	-
	AUC	0.812	0.829	0.834	0.739	0.752	0.788
	CI (95%)	[0.716,0.908]	[0.738,0.920]	[0.741,0.926]	[0.620,0.858]	[0.633,0.872]	[0.685,0.892]
	p csa/csanorm	0.540	0.564	0.961	0.540	0.594	0.748
nCSA <sub>C1-C7</sub>	P <sub>C1-2 / C1-7</sub>	-	0.875	-	-	0.370	-
	P brain / cord	0.397	-	-	0.651	-	-
	P NQL/ASM	0.082	0.077	0.179	-	-	-
	AUC	0.812	0.825	0.834	0.774	0.774	0.799
	CI (95%)	[0.716,0.907]	[0.732,0.918]	[0.741,0.927]	[0.664,0.884]	[0.666,0.882]	[0.700,0.899]
	p <sub>CSA/CSAnorm</sub>	0.665	0.701	0.961	0.456	0.570	0.729
nCSA <sub>C3-area</sub>	P <sub>C1-2 / C1-7</sub>	-	0.616	-	-	0.370	-
	P brain / cord	0.386	-	-	0.961	-	-
	P NQL / ASM	0.299	0.290	0.179	-	-	-

# Supplementary Table S9: Recommendations for CSA quantification in the cervical cord of patients with MS

CSA quantification in the cervical spinal cord	Recomme	endation	Alteri	native	
MRI acquisition type	Dedicated cervical cord MRI	with isotropic 3D-T1w	Brain MRI incl. sagittal 3D_T1w covering the upper cervical cord		
Pros and Cons	Pro: *enable measurements at all cervical cord levels; Con: * long acquisition times for brain & cord MRI  * no significant differences between by brain MRI compared with cord MC Con: * limited to upper cervical cord.			es between CSA at C1-2 vith cord MRI	
CSA in whole cervical cord or upper cervical cord?	Whole cervical cord (C1-7) w	ith cord MRI	Upper cervical cord section or cord MRI	ons (e.g. C1-2) with brain	
Pros and Cons	<b>Pro:</b> * Best discrimination be subtypes; strongest correlat <b>Con:</b> * Longer acquisition tim	ions with EDSS scores.	Pro: *Good discrimination between MS and HC at C1-2 level; Con: * Slightly worse discrimination between rMS and pMS than whole cervical cord measurements;		
CSA normalization	Use spine skeletal normaliza C2 vertebrae recommended; vertebrae	_	According to published literature (not part of our study): brain intracranial cavity volume might be used for normalization, if brain MRI and automated analysis pipelines are available.		
Pros and Cons	MS subtypes and correlation	s discrimination between s with EDSS; ne MRI derived number;	Potential Pros and Cons:  Pro: * automated calculation in brain analysis pipelines;  Con: * volumetric brain analysis and brain MRI necessary		
Image analysis software	Active surface (ASM)	NQL	SCT_PS SCT_DS		
Suitability dependent on sample size	Semiautomated	Semiautomated	Fully automated Fully automated		